

Measurement of partial branching fractions of inclusive charmless B meson decays to K^+ , K^0 , and π^+

P. del Amo Sanchez,¹ J. P. Lees,¹ V. Poireau,¹ E. Prencipe,¹ V. Tisserand,¹ J. Garra Tico,² E. Grauges,² M. Martinelli,^{3a,3b} D. A. Milanes,^{3a} A. Palano,^{3a,3b} M. Pappagallo,^{3a,3b} G. Eigen,⁴ B. Stugu,⁴ L. Sun,⁴ D. N. Brown,⁵ L. T. Kerth,⁵ Yu. G. Kolomensky,⁵ G. Lynch,⁵ I. L. Osipenkov,⁵ H. Koch,⁶ T. Schroeder,⁶ D. J. Asgeirsson,⁷ C. Hearty,⁷ T. S. Mattison,⁷ J. A. McKenna,⁷ A. Khan,⁸ V. E. Blinov,⁹ A. R. Buzykaev,⁹ V. P. Druzhinin,⁹ V. B. Golubev,⁹ E. A. Kravchenko,⁹ A. P. Onuchin,⁹ S. I. Serednyakov,⁹ Yu. I. Skovpen,⁹ E. P. Solodov,⁹ K. Yu. Todyshev,⁹ A. N. Yushkov,⁹ M. Bondioli,¹⁰ S. Curry,¹⁰ D. Kirkby,¹⁰ A. J. Lankford,¹⁰ M. Mandelkern,¹⁰ E. C. Martin,¹⁰ D. P. Stoker,¹⁰ H. Atmacan,¹¹ J. W. Gary,¹¹ F. Liu,¹¹ O. Long,¹¹ G. M. Vitug,¹¹ C. Campagnari,¹² T. M. Hong,¹² D. Kovalskyi,¹² J. D. Richman,¹² C. A. West,¹² A. M. Eisner,¹³ C. A. Heusch,¹³ J. Kroseberg,¹³ W. S. Lockman,¹³ A. J. Martinez,¹³ T. Schalk,¹³ B. A. Schumm,¹³ A. Seiden,¹³ L. O. Winstrom,¹³ C. H. Cheng,¹⁴ D. A. Doll,¹⁴ B. Echenard,¹⁴ D. G. Hitlin,¹⁴ P. Ongmongkolkul,¹⁴ F. C. Porter,¹⁴ A. Y. Rakitin,¹⁴ R. Andreassen,¹⁵ M. S. Dubrovin,¹⁵ B. T. Meadows,¹⁵ M. D. Sokoloff,¹⁵ F. Blanc,¹⁶ P. C. Bloom,¹⁶ W. T. Ford,¹⁶ A. Gaz,¹⁶ M. Nagel,¹⁶ U. Nauenberg,¹⁶ J. G. Smith,¹⁶ S. R. Wagner,¹⁶ R. Ayad,^{17,*} W. H. Toki,¹⁷ H. Jasper,¹⁸ A. Petzold,¹⁸ B. Spaan,¹⁸ M. J. Kobel,¹⁹ K. R. Schubert,¹⁹ R. Schwierz,¹⁹ D. Bernard,²⁰ M. Verderi,²⁰ P. J. Clark,²¹ S. Playfer,²¹ J. E. Watson,²¹ M. Andreotti,^{22a,22b} D. Bettoni,^{22a} C. Bozzi,^{22a} R. Calabrese,^{22a,22b} A. Cecchi,^{22a,22b} G. Cibinetto,^{22a,22b} E. Fioravanti,^{22a,22b} P. Franchini,^{22a,22b} I. Garzia,^{22a,22b} E. Luppi,^{22a,22b} M. Menerato,^{22a,22b} M. Negrini,^{22a,22b} A. Petrella,^{22a,22b} L. Piemontese,^{22a} R. Baldini-Ferrolli,²³ A. Calcaterra,²³ R. de Sangro,²³ G. Finocchiaro,²³ M. Nicolaci,²³ S. Pacetti,²³ P. Patteri,²³ I. M. Peruzzi,^{23,†} M. Piccolo,²³ M. Rama,²³ A. Zallo,²³ R. Contri,^{24a,24b} E. Guido,^{24a,24b} M. Lo Vetere,^{24a,24b} M. R. Monge,^{24a,24b} S. Passaggio,^{24a} C. Patrignani,^{24a,24b} E. Robutti,^{24a} B. Bhuyan,²⁵ V. Prasad,²⁵ C. L. Lee,²⁶ M. Morii,²⁶ A. J. Edwards,²⁷ A. Adametz,²⁸ J. Marks,²⁸ U. Uwer,²⁸ F. U. Bernlochner,²⁹ M. Ebert,²⁹ H. M. Lacker,²⁹ T. Lueck,²⁹ A. Volk,²⁹ P. D. Dauncey,³⁰ M. Tibbetts,³⁰ P. K. Behera,³¹ U. Mallik,³¹ C. Chen,³² J. Cochran,³² H. B. Crawley,³² W. T. Meyer,³² S. Prell,³² E. I. Rosenberg,³² A. E. Rubin,³² A. V. Gritsan,³³ Z. J. Guo,³³ N. Arnaud,³⁴ M. Davier,³⁴ D. Derkach,³⁴ J. Firmino da Costa,³⁴ G. Grosdidier,³⁴ F. Le Diberder,³⁴ A. M. Lutz,³⁴ B. Malaescu,³⁴ A. Perez,³⁴ P. Roudeau,³⁴ M. H. Schune,³⁴ J. Serrano,³⁴ V. Sordini,^{34,‡} A. Stocchi,³⁴ L. Wang,³⁴ G. Wormser,³⁴ D. J. Lange,³⁵ D. M. Wright,³⁵ I. Bingham,³⁶ C. A. Chavez,³⁶ J. P. Coleman,³⁶ J. R. Fry,³⁶ E. Gabathuler,³⁶ D. E. Hutchcroft,³⁶ D. J. Payne,³⁶ C. Touramanis,³⁶ A. J. Bevan,³⁷ F. Di Lodovico,³⁷ R. Sacco,³⁷ M. Sigamani,³⁷ G. Cowan,³⁸ S. Paramesvaran,³⁸ A. C. Wren,³⁸ D. N. Brown,³⁹ C. L. Davis,³⁹ A. G. Denig,⁴⁰ M. Fritsch,⁴⁰ W. Gradl,⁴⁰ A. Hafner,⁴⁰ K. E. Alwyn,⁴¹ D. Bailey,⁴¹ R. J. Barlow,⁴¹ G. Jackson,⁴¹ G. D. Lafferty,⁴¹ J. Anderson,⁴² R. Cenci,⁴² A. Jawahery,⁴² D. A. Roberts,⁴² G. Simi,⁴² J. M. Tuggle,⁴² C. Dallapiccola,⁴³ E. Salvati,⁴³ R. Cowan,⁴⁴ D. Dujmic,⁴⁴ G. Sciolla,⁴⁴ M. Zhao,⁴⁴ D. Lindemann,⁴⁵ P. M. Patel,⁴⁵ S. H. Robertson,⁴⁵ M. Schram,⁴⁵ P. Biassoni,^{46a,46b} A. Lazzaro,^{46a,46b} V. Lombardo,^{46a} F. Palombo,^{46a,46b} S. Stracka,^{46a,46b} L. Cremaldi,⁴⁷ R. Godang,^{47,§} R. Kroeger,⁴⁷ P. Sonnek,⁴⁷ D. J. Summers,⁴⁷ X. Nguyen,⁴⁸ M. Simard,⁴⁸ P. Taras,⁴⁸ G. De Nardo,^{49a,49b} D. Monorchio,^{49a,49b} G. Onorato,^{49a,49b} C. Sciacca,^{49a,49b} G. Raven,⁵⁰ H. L. Snoek,⁵⁰ C. P. Jessop,⁵¹ K. J. Knoepfel,⁵¹ J. M. LoSecco,⁵¹ W. F. Wang,⁵¹ L. A. Corwin,⁵² K. Honscheid,⁵² R. Kass,⁵² N. L. Blount,⁵³ J. Brau,⁵³ R. Frey,⁵³ O. Igonkina,⁵³ J. A. Kolb,⁵³ R. Rahmat,⁵³ N. B. Sinev,⁵³ D. Strom,⁵³ J. Strube,⁵³ E. Torrence,⁵³ G. Castelli,^{54a,54b} E. Feltresi,^{54a,54b} N. Gagliardi,^{54a,54b} M. Margoni,^{54a} M. Morandin,^{54a} M. Posocco,^{54a} M. Rotondo,^{54a} F. Simonetto,^{54a,54b} R. Stroili,^{54a,54b} E. Ben-Haim,⁵⁵ M. Bomben,⁵⁵ G. R. Bonneaud,⁵⁵ H. Briand,⁵⁵ G. Calderini,⁵⁵ J. Chauveau,⁵⁵ O. Hamon,⁵⁵ Ph. Leruste,⁵⁵ G. Marchiori,⁵⁵ J. Ocariz,⁵⁵ J. Prendki,⁵⁵ S. Sitt,⁵⁵ M. Biasini,^{56a,56b} E. Manoni,^{56a,56b} A. Rossi,^{56a,56b} C. Angelini,^{57a,57b} G. Batignani,^{57a,57b} S. Bettarini,^{57a,57b} M. Carpinelli,^{57a,57b,||} G. Casarosa,^{57a,57b} A. Cervelli,^{57a,57b} F. Forti,^{57a,57b} M. A. Giorgi,^{57a,57b} A. Lusiani,^{57a,57c} N. Neri,^{57a,57b} E. Paoloni,^{57a,57b} G. Rizzo,^{57a,57b} J. J. Walsh,^{57a} D. Lopes Pegna,⁵⁸ C. Lu,⁵⁸ J. Olsen,⁵⁸ A. J. S. Smith,⁵⁸ A. V. Telnov,⁵⁸ F. Anulli,^{59a} E. Baracchini,^{59a,59b} G. Cavoto,^{59a} R. Faccini,^{59a,59b} F. Ferrarotto,^{59a} F. Ferroni,^{59a,59b} M. Gaspero,^{59a,59b} L. Li Gioi,^{59a} M. A. Mazzoni,^{59a} G. Piredda,^{59a} F. Renga,^{59a,59b} C. Buenger,⁶⁰ T. Hartmann,⁶⁰ T. Leddig,⁶⁰ H. Schröder,⁶⁰ R. Waldi,⁶⁰ T. Adye,⁶¹ E. O. Olaiya,⁶¹ F. F. Wilson,⁶¹ S. Emery,⁶² G. Hamel de Monchenault,⁶² G. Vasseur,⁶² Ch. Yèche,⁶² M. T. Allen,⁶³ D. Aston,⁶³ D. J. Bard,⁶³ R. Bartoldus,⁶³ J. F. Benitez,⁶³ C. Cartaro,⁶³ M. R. Convery,⁶³ J. Dorfan,⁶³ G. P. Dubois-Felsmann,⁶³ W. Dunwoodie,⁶³ R. C. Field,⁶³ M. Franco Sevilla,⁶³ B. G. Fulsom,⁶³ A. M. Gabareen,⁶³ M. T. Graham,⁶³ P. Grenier,⁶³ C. Hast,⁶³ W. R. Innes,⁶³ M. H. Kelsey,⁶³ H. Kim,⁶³ P. Kim,⁶³ M. L. Kocian,⁶³ D. W. G. S. Leith,⁶³ P. Lewis,⁶³ S. Li,⁶³ B. Lindquist,⁶³ S. Luitz,⁶³ V. Luth,⁶³ H. L. Lynch,⁶³ D. B. MacFarlane,⁶³ D. R. Muller,⁶³ H. Neal,⁶³ S. Nelson,⁶³ C. P. O'Grady,⁶³ I. Ofte,⁶³ M. Perl,⁶³ T. Pulliam,⁶³ B. N. Ratcliff,⁶³ A. Roodman,⁶³ A. A. Salnikov,⁶³ V. Santoro,⁶³ R. H. Schindler,⁶³ J. Schwiening,⁶³ A. Snyder,⁶³ D. Su,⁶³ M. K. Sullivan,⁶³ S. Sun,⁶³

K. Suzuki,⁶³ J. M. Thompson,⁶³ J. Va'vra,⁶³ A. P. Wagner,⁶³ M. Weaver,⁶³ W. J. Wisniewski,⁶³ M. Wittgen,⁶³ D. H. Wright,⁶³ H. W. Wulsin,⁶³ A. K. Yarritu,⁶³ C. C. Young,⁶³ V. Ziegler,⁶³ X. R. Chen,⁶⁴ W. Park,⁶⁴ M. V. Purohit,⁶⁴ R. M. White,⁶⁴ J. R. Wilson,⁶⁴ A. Randle-Conde,⁶⁵ S. J. Sekula,⁶⁵ M. Bellis,⁶⁶ P. R. Burchat,⁶⁶ T. S. Miyashita,⁶⁶ S. Ahmed,⁶⁷ M. S. Alam,⁶⁷ J. A. Ernst,⁶⁷ B. Pan,⁶⁷ M. A. Saeed,⁶⁷ S. B. Zain,⁶⁷ N. Guttman,⁶⁸ A. Soffer,⁶⁸ P. Lund,⁶⁹ S. M. Spanier,⁶⁹ R. Eckmann,⁷⁰ J. L. Ritchie,⁷⁰ A. M. Ruland,⁷⁰ C. J. Schilling,⁷⁰ R. F. Schwitters,⁷⁰ B. C. Wray,⁷⁰ J. M. Izen,⁷¹ X. C. Lou,⁷¹ F. Bianchi,^{72a,72b} D. Gamba,^{72a,72b} M. Pelliccioni,^{72a,72b} L. Lanceri,^{73a,73b} L. Vitale,^{73a,73b} N. Lopez-March,⁷⁴ F. Martinez-Vidal,⁷⁴ A. Oyanguren,⁷⁴ H. Ahmed,⁷⁵ J. Albert,⁷⁵ Sw. Banerjee,⁷⁵ H. H. F. Choi,⁷⁵ K. Hamano,⁷⁵ G. J. King,⁷⁵ R. Kowalewski,⁷⁵ M. J. Lewczuk,⁷⁵ C. Lindsay,⁷⁵ I. M. Nugent,⁷⁵ J. M. Roney,⁷⁵ R. J. Sobie,⁷⁵ T. J. Gershon,⁷⁶ P. F. Harrison,⁷⁶ T. E. Latham,⁷⁶ E. M. T. Puccio,⁷⁶ H. R. Band,⁷⁷ S. Dasu,⁷⁷ K. T. Flood,⁷⁷ Y. Pan,⁷⁷ R. Prepost,⁷⁷ C. O. Vuosalo,⁷⁷ and S. L. Wu⁷⁷

(The *BABAR* Collaboration)

¹*Laboratoire d'Annecy-le-Vieux de Physique des Particules (LAPP), Université de Savoie, CNRS/IN₂P₃, F-74941 Annecy-Le-Vieux, France*

²*Universitat de Barcelona, Facultat de Física, Departament ECM, E-08028 Barcelona, Spain*

^{3a}*INFN Sezione di Bari, I-70126 Bari, Italy*

^{3b}*Dipartimento di Fisica Università di Bari, I-70126 Bari, Italy*

⁴*University of Bergen, Institute of Physics, N-5007 Bergen, Norway*

⁵*Lawrence Berkeley National Laboratory and University of California, Berkeley, California 94720, USA*

⁶*Ruhr Universität Bochum, Institut für Experimentalphysik 1, D-44780 Bochum, Germany*

⁷*University of British Columbia, Vancouver, British Columbia, Canada V6T 1Z1*

⁸*Brunel University, Uxbridge, Middlesex UB8 3PH, United Kingdom*

⁹*Budker Institute of Nuclear Physics, Novosibirsk 630090, Russia*

¹⁰*University of California at Irvine, Irvine, California 92697, USA*

¹¹*University of California at Riverside, Riverside, California 92521, USA*

¹²*University of California at Santa Barbara, Santa Barbara, California 93106, USA*

¹³*University of California at Santa Cruz, Institute for Particle Physics, Santa Cruz, California 95064, USA*

¹⁴*California Institute of Technology, Pasadena, California 91125, USA*

¹⁵*University of Cincinnati, Cincinnati, Ohio 45221, USA*

¹⁶*University of Colorado, Boulder, Colorado 80309, USA*

¹⁷*Colorado State University, Fort Collins, Colorado 80523, USA*

¹⁸*Technische Universität Dortmund, Fakultät Physik, D-44221 Dortmund, Germany*

¹⁹*Technische Universität Dresden, Institut für Kern- und Teilchenphysik, D-01062 Dresden, Germany*

²⁰*Laboratoire Leprince-Ringuet, CNRS/IN₂P₃, Ecole Polytechnique, F-91128 Palaiseau, France*

²¹*University of Edinburgh, Edinburgh EH9 3JZ, United Kingdom*

^{22a}*INFN Sezione di Ferrara, I-44100 Ferrara, Italy*

^{22b}*Dipartimento di Fisica, Università di Ferrara, I-44100 Ferrara, Italy*

²³*INFN Laboratori Nazionali di Frascati, I-00044 Frascati, Italy*

^{24a}*INFN Sezione di Genova, I-16146 Genova, Italy*

^{24b}*Dipartimento di Fisica, Università di Genova, I-16146 Genova, Italy*

²⁵*Indian Institute of Technology Guwahati, Guwahati, Assam, 781 039, India*

²⁶*Harvard University, Cambridge, Massachusetts 02138, USA*

²⁷*Harvey Mudd College, Claremont, California 91711*

²⁸*Universität Heidelberg, Physikalisches Institut, Philosophenweg 12, D-69120 Heidelberg, Germany*

²⁹*Humboldt-Universität zu Berlin, Institut für Physik, Newtonstr. 15, D-12489 Berlin, Germany*

³⁰*Imperial College London, London, SW7 2AZ, United Kingdom*

³¹*University of Iowa, Iowa City, Iowa 52242, USA*

³²*Iowa State University, Ames, Iowa 50011-3160, USA*

³³*Johns Hopkins University, Baltimore, Maryland 21218, USA*

³⁴*Laboratoire de l'Accélérateur Linéaire, IN₂P₃/CNRS et Université Paris-Sud 11, Centre Scientifique d'Orsay, B. P. 34, F-91898 Orsay Cedex, France*

³⁵*Lawrence Livermore National Laboratory, Livermore, California 94550, USA*

³⁶*University of Liverpool, Liverpool L69 7ZE, United Kingdom*

³⁷*Queen Mary, University of London, London, E1 4NS, United Kingdom*

³⁸*University of London, Royal Holloway and Bedford New College, Egham, Surrey TW20 0EX, United Kingdom*

³⁹*University of Louisville, Louisville, Kentucky 40292, USA*

⁴⁰*Johannes Gutenberg-Universität Mainz, Institut für Kernphysik, D-55099 Mainz, Germany*

- ⁴¹University of Manchester, Manchester M13 9PL, United Kingdom
⁴²University of Maryland, College Park, Maryland 20742, USA
⁴³University of Massachusetts, Amherst, Massachusetts 01003, USA
⁴⁴Massachusetts Institute of Technology, Laboratory for Nuclear Science, Cambridge, Massachusetts 02139, USA
⁴⁵McGill University, Montréal, Québec, Canada H3A 2T8
^{46a}INFN Sezione di Milano, I-20133 Milano, Italy
^{46b}Dipartimento di Fisica, Università di Milano, I-20133 Milano, Italy
⁴⁷University of Mississippi, University, Mississippi 38677, USA
⁴⁸Université de Montréal, Physique des Particules, Montréal, Québec, Canada H3C 3J7
^{49a}INFN Sezione di Napoli, I-80126 Napoli, Italy
^{49b}Dipartimento di Scienze Fisiche, Università di Napoli Federico II, I-80126 Napoli, Italy
⁵⁰NIKHEF, National Institute for Nuclear Physics and High Energy Physics, NL-1009 DB Amsterdam, The Netherlands
⁵¹University of Notre Dame, Notre Dame, Indiana 46556, USA
⁵²Ohio State University, Columbus, Ohio 43210, USA
⁵³University of Oregon, Eugene, Oregon 97403, USA
^{54a}INFN Sezione di Padova, I-35131 Padova, Italy
^{54b}Dipartimento di Fisica, Università di Padova, I-35131 Padova, Italy
⁵⁵Laboratoire de Physique Nucléaire et de Hautes Energies, IN₂P₃/CNRS, Université Pierre et Marie Curie-Paris6, Université Denis Diderot-Paris7, F-75252 Paris, France
^{56a}INFN Sezione di Perugia, I-06100 Perugia, Italy
^{56b}Dipartimento di Fisica, Università di Perugia, I-06100 Perugia, Italy
^{57a}INFN Sezione di Pisa, I-56127 Pisa, Italy
^{57b}Dipartimento di Fisica, Università di Pisa, I-56127 Pisa, Italy
^{57c}Scuola Normale Superiore di Pisa, I-56127 Pisa, Italy
⁵⁸Princeton University, Princeton, New Jersey 08544, USA
^{59a}INFN Sezione di Roma, I-00185 Roma, Italy
^{59b}Dipartimento di Fisica, Università di Roma La Sapienza, I-00185 Roma, Italy
⁶⁰Universität Rostock, D-18051 Rostock, Germany
⁶¹Rutherford Appleton Laboratory, Chilton, Didcot, Oxon, OX11 0QX, United Kingdom
⁶²CEA, Irfu, SPP, Centre de Saclay, F-91191 Gif-sur-Yvette, France
⁶³SLAC National Accelerator Laboratory, Stanford, California 94309 USA
⁶⁴University of South Carolina, Columbia, South Carolina 29208, USA
⁶⁵Southern Methodist University, Dallas, Texas 75275, USA
⁶⁶Stanford University, Stanford, California 94305-4060, USA
⁶⁷State University of New York, Albany, New York 12222, USA
⁶⁸Tel Aviv University, School of Physics and Astronomy, Tel Aviv, 69978, Israel
⁶⁹University of Tennessee, Knoxville, Tennessee 37996, USA
⁷⁰University of Texas at Austin, Austin, Texas 78712, USA
⁷¹University of Texas at Dallas, Richardson, Texas 75083, USA
^{72a}INFN Sezione di Torino, I-10125 Torino, Italy
^{72b}Dipartimento di Fisica Sperimentale, Università di Torino, I-10125 Torino, Italy
^{73a}INFN Sezione di Trieste, I-34127 Trieste, Italy
^{73b}Dipartimento di Fisica, Università di Trieste, I-34127 Trieste, Italy
⁷⁴IFIC, Universitat de Valencia-CSIC, E-46071 Valencia, Spain
⁷⁵University of Victoria, Victoria, British Columbia, Canada V8W 3P6
⁷⁶Department of Physics, University of Warwick, Coventry CV4 7AL, United Kingdom
⁷⁷University of Wisconsin, Madison, Wisconsin 53706, USA

(Received 23 December 2010; published 14 February 2011)

We present measurements of partial branching fractions of $B \rightarrow K^+ X$, $B \rightarrow K^0 X$, and $B \rightarrow \pi^+ X$, where X denotes any accessible final state above the endpoint for B decays to charmed mesons, specifically for momenta of the candidate hadron greater than 2.34 (2.36) GeV for kaons (pions) in the B rest frame. These measurements are sensitive to potential new-physics particles which could enter the $b \rightarrow s(d)$ loop transitions. The analysis is performed on a data sample consisting of $383 \times 10^6 B\bar{B}$ pairs

*Now at Temple University, Philadelphia, PA 19122, USA

†Also with Università di Perugia, Dipartimento di Fisica, Perugia, Italy

‡Also with Università di Roma La Sapienza, I-00185 Roma, Italy

§Present address: University of South Alabama, Mobile, AL 36688, USA

||Also with Università di Sassari, Sassari, Italy

collected with the *BABAR* detector at the PEP-II e^+e^- asymmetric energy collider. We observe the inclusive $B \rightarrow \pi^+ X$ process, and we set upper limits for $B \rightarrow K^+ X$ and $B \rightarrow K^0 X$. Our results for these inclusive branching fractions are consistent with those of known exclusive modes, and exclude large enhancements due to sources of new physics.

DOI: 10.1103/PhysRevD.83.031103

PACS numbers: 13.25.Hw, 11.30.Er, 12.15.Ji

B mesons decay predominantly to charmed mesons through the tree level process $b \rightarrow c$, while the tree amplitude $b \rightarrow u$ and the one-loop processes $b \rightarrow s$ and $b \rightarrow d$ are strongly suppressed. In the standard model (SM), the inclusive branching fraction of B mesons to charmless final states is of the order of 2% [1]. Particles associated with physics beyond the SM, such as supersymmetric partners of SM particles, could enter the loop amplitudes while leaving the tree level processes nearly unaffected, making a sizable enhancement of the inclusive $b \rightarrow s(d)g$ (where g denotes a gluon) branching fraction possible [2,3]. Additionally, since semi-inclusive processes are usually affected by smaller hadronic uncertainties than those that arise in calculations for exclusive final states, these decays can be sensitive to nonperturbative amplitudes, such as charming penguins [4].

An interesting theoretical mechanism that can modify the SM prediction is provided by the Randall-Sundrum framework, in particular, from the Warped Top-Condensation Model where a radion field ϕ is postulated. In the case where $1 < m(\phi) < 3.7$ GeV, the radion would decay dominantly to gluons, thus enhancing the rate of the charmless B decays through the process $b \rightarrow s\phi$. In such a model the $b \rightarrow s$ inclusive decay rate could be enhanced by an order of magnitude with respect to the SM predictions [5].

Historically, an enhancement of charmless B decays had been postulated [6] to explain the deficit of $b \rightarrow c$ processes observed by the ARGUS and CLEO experiments [7]. Later measurements and refined theoretical calculations established that no significant discrepancy was present [8]. Inclusive $b \rightarrow sg$ decays have been searched for by the ARGUS, CLEO, and DELPHI collaborations [9]. None of these experiments has found a statistically significant signal and only upper limits in agreement with theoretical expectations were set.

In this paper we present measurements of partial branching fractions of inclusive charmless B -meson decays. The signature of these decays is the presence of a light meson (K^+ , K_S^0 , or π^+ [10]) with momentum beyond the kinematic endpoint for B decays to charmed mesons, measured recoiling against a fully reconstructed B meson. It is possible to compare our results with the inclusive branching fraction of $b \rightarrow s\gamma$ in the same kinematical region and with some recent theoretical predictions [4] based on Soft Collinear Effective Theory.

The measurement is performed on a data sample collected by the *BABAR* detector [11], operated at the asymmetric energy e^+e^- PEP-II collider at the SLAC National

Accelerator Laboratory. We use 347 fb^{-1} (equivalent to $383 \times 10^6 B\bar{B}$ pairs) collected at a center-of-mass energy \sqrt{s} corresponding to the mass of the $\Upsilon(4S)$ resonance, which predominantly decays to charged or neutral $B\bar{B}$ pairs; a smaller sample (37 fb^{-1}) of data collected at an energy of 40 MeV below the $\Upsilon(4S)$ peak is used to study the background originating from continuum $e^+e^- \rightarrow q\bar{q}$ ($q = u, d, s, c$) processes.

In order to suppress the potentially overwhelming background from continuum events, we fully reconstruct one of the two B mesons (denoted by B_{reco}) and search for a high momentum light hadron (K^+ , K_S^0 , or π^+) among the decay products of the other B (B_{sig}). The full reconstruction of the B_{reco} candidate allows us to determine the four-momentum of B_{sig} precisely. In order to suppress backgrounds arising from the dominant B decays to charmed mesons, we require the light meson's momentum p^* in the B_{sig} rest frame to be greater than 2.34 (2.36) GeV in the kaon (pion) case; this corresponds to a system, recoiling against the candidate hadron, of mass less than 1.69 (1.71) GeV. The separation of K^+ from π^+ candidates is based on the Cherenkov angle measured in the Detector of Internally Reflected Cherenkov light.

The B_{reco} is reconstructed in the decays $B \rightarrow D^{(*)}Y^\pm$, where Y^\pm is a combination of hadrons containing one, three, or five charged kaons or pions, up to two neutral pions, and at most two $K_S^0 \rightarrow \pi^+\pi^-$. We reconstruct $D^{*-} \rightarrow \bar{D}^0\pi^-$; $\bar{D}^{*0} \rightarrow \bar{D}^0\pi^0$; $\bar{D}^0 \rightarrow K^+\pi^-$, $K^+\pi^-\pi^0$, $K^+\pi^-\pi^-\pi^+$, $K_S^0\pi^+\pi^-$; and $D^- \rightarrow K^+\pi^-\pi^-$, $K^+\pi^-\pi^-\pi^0$, $K_S^0\pi^-$, $K_S^0\pi^-\pi^0$, $K_S^0\pi^-\pi^-\pi^+$. We define the purity of a particular mode as $S/(S+B)$, where S (B) denotes the number of signal (background) events; we use only the 186 B_{reco} final states with purity, measured in data control samples, greater than 0.2. When more than one B_{reco} candidate is found in an event, we retain the one with the decay mode having the highest purity; the overall purity of our selected sample is approximately 0.45.

Two kinematic variables characterize correctly reconstructed B candidates: the energy-substituted mass $m_{\text{ES}} \equiv \sqrt{s/4 - \mathbf{p}_B^2}$ and the energy difference $\Delta E \equiv E_B - \sqrt{s}/2$, where (E_B, \mathbf{p}_B) is the B -meson four-momentum in the $\Upsilon(4S)$ rest frame. For the B_{reco} candidate, we select events with $5.2500 < m_{\text{ES}} < 5.2893$ GeV and we apply a mode-dependent cut on ΔE . Additional background rejection is provided by the angle θ_T , defined as the angle between the thrust axis of the B_{reco} candidate decay products and the

rest of the event. For continuum events $|\cos\theta_T|$ peaks sharply at 1, while $B\bar{B}$ events exhibit a uniform distribution. We select events with $|\cos\theta_T| < 0.9$.

Finally, we combine into a Fisher discriminant \mathcal{F} four variables sensitive to the event shape and the production dynamics: the polar angles with respect to the beam axis in the $Y(4S)$ frame of the B_{reco} candidate momentum and of the B_{reco} thrust axis, and the zeroth and second angular moments $L_{0,2}$ of the energy flow. The moments are defined by $L_j = \sum_i p_i \times |\cos\theta_i|^j$, where i labels a charged or neutral candidate not originating from the decay of the B_{reco} , θ_i is the angle with respect to the B_{reco} thrust axis, and p_i is its momentum.

The branching fractions we are measuring are normalized to the number of fully reconstructed $B\bar{B}$ events present in our sample. We determine the $B\bar{B}$ yield (over the $q\bar{q}$ continuum background) through a maximum likelihood fit to the variables m_{ES} and \mathcal{F} . The probability density function (PDF) of m_{ES} for the $B\bar{B}$ category is the sum of two components: two Gaussian functions centered on the mass of the B parameterize the correctly reconstructed B candidates, while an ARGUS [12] function describes the misreconstructed B decays. For the continuum we use only an ARGUS function. For the \mathcal{F} variable we use the sum of a bifurcated Gaussian with a Gaussian for both $B\bar{B}$ and $q\bar{q}$. Besides the yields of the two components ($B\bar{B}$ and $q\bar{q}$), the ARGUS exponent for the $q\bar{q}$ component and the fraction of correctly reconstructed $B\bar{B}$ events are free. We split the data sample into four subsamples characterized by different purity ranges of the B_{reco} candidates. The ARGUS exponent and the fraction of $B\bar{B}$ events peaking in m_{ES} are allowed to take different values among these categories. Figure 1 shows the projection over the m_{ES} variable of

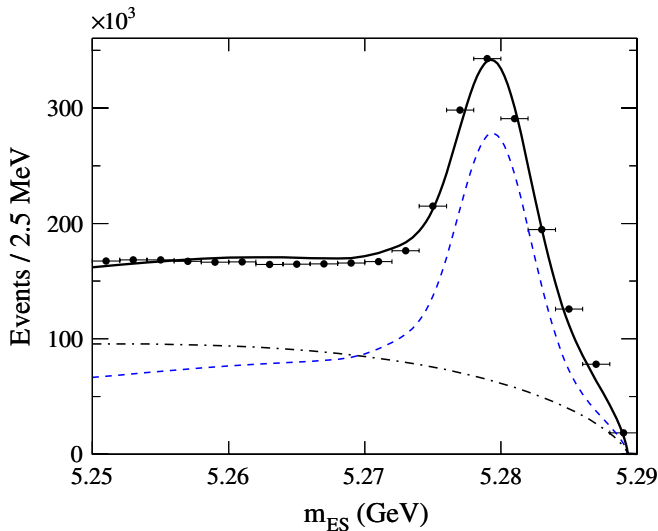


FIG. 1 (color online). Projection of the m_{ES} variable for the B_{reco} sample; the dashed line represents the $B\bar{B}$ component, the dot-dashed is the continuum background, and the solid line is the sum of the two components.

this fit. The $B\bar{B}$ yield is $(2.0902 \pm 0.0020) \times 10^6$ $B\bar{B}$ events. By repeating the fit on the subsamples with different purities and using different parameterizations for the PDFs, we estimate the systematic uncertainty on the $B\bar{B}$ yield to be 5%.

We assign to B_{sig} all the charged and neutral particles that do not belong to the B_{reco} candidate and require $5.1000 < m_{\text{ES}}(B_{\text{sig}}) < 5.2893$ GeV. This loose cut suppresses background events in which a significant amount of energy and momentum is lost. We suppress $b \rightarrow c$ semileptonic decays by rejecting events where an electron or muon candidate is present. We also veto events in which a D^0 , D^+ , or D_s^+ candidate, with a mass within 30 MeV of the nominal value, is found.

We require that a K^+ , K_S^0 , or π^+ candidate with $p^* > 1.8$ GeV be present on the signal side. The distance of closest approach for K^+ and π^+ candidates must be less than 3 standard deviations from the B_{sig} decay vertex. K_S^0 candidates are reconstructed in the $\pi^+\pi^-$ final state, with requirements that the vertex probability of the two tracks be greater than 10^{-4} , that the flight length be greater than 3 times its uncertainty, and that their mass satisfy $0.486 < m_{\pi^+\pi^-} < 0.510$ GeV.

We extract the signal yields from a maximum likelihood fit to the three variables $m_{\text{ES}}(B_{\text{reco}})$, \mathcal{F} , and p^* . For the K^+ and π^+ samples we also measure the direct CP asymmetry $\mathcal{A}_{\text{ch}} \equiv (\Gamma^- - \Gamma^+)/(\Gamma^- + \Gamma^+)$, where the superscript to the decay width Γ refers to the charge of the light hadron. Our fits have three components: signal, $b \rightarrow c$ background, and continuum background. For each of these categories j we define probability density functions $\mathcal{P}_j(x)$ for the variable x , with the resulting likelihood:

$$\mathcal{P}_j = \mathcal{P}_j(m_{\text{ES}})\mathcal{P}_j(\mathcal{F})\mathcal{P}_j(p^*), \quad (1)$$

$$\mathcal{L} = \frac{e^{-\sum_j Y_j}}{N!} \prod_{i=1}^N \sum_j Y_j \mathcal{P}_j^i, \quad (2)$$

where \mathcal{P}_j^i is \mathcal{P}_j evaluated for event i , Y_j is the yield for category j , and N is the number of events entering the fit. We assume the PDFs for each variable to be uncorrelated in the signal and $b \rightarrow c$ components (a correlation in the continuum component is handled as discussed below). We check this assumption by means of Monte Carlo (MC) experiments [13], in which signal and $b \rightarrow c$ events are taken from fully simulated event samples and the continuum background is generated from the PDFs. In the extraction of the signal yields, we correct for the small biases we observe in these ensembles. The PDFs are extracted by fitting MC samples, where the charmless decays are separated from $b \rightarrow c$ background using information at the generator level.

Signal and $b \rightarrow c$ events share the same PDFs for the m_{ES} and \mathcal{F} variables which are only effective to separate $B\bar{B}$ events from the continuum; the fit distinguishes

between charmed and charmless B decays by exploiting the differences in the p^* distributions. The p^* distribution is parameterized by the sum of a Gaussian with an ARGUS function for the signal, by the sum of an exponential and a Gaussian for the $q\bar{q}$ component, and by the sum of three, one, or five Gaussians for the $b \rightarrow c$ background in the K^+ , K_S^0 and π^+ samples, respectively. The latter parameterize the broad component(s) of the $b \rightarrow c$ background and the peaking components corresponding to the $B \rightarrow D^{(**)}h$, ($h = K^+, K_S^0$ or π^+) decays, all of which are evident in the π^+ sample (see Fig. 2). Similarly, the Gaussian component of the signal p^* PDF accounts for the dominant two-body decays (mainly $B \rightarrow \eta'K$), while the broad component describes the sum of the other contributions. The splitting of the data into subsamples based on the purity and the charge of the B_{reco} candidates allows differences in the background distributions to be accommodated in the fit by allowing the parameters most sensitive to these variations to take different values in each subsample.

The fit is performed through an iterative procedure. In the first step we fix the signal yield to the predictions of the MC and fit the $p^* > 1.8$ GeV sample, leaving free to vary the most important parameters of the background such as the normalization of the peaking components in the $b \rightarrow c$ background, the width of the broad components, and the exponent of the ARGUS function. This step is aimed at determining the shape and the normalization of the $b \rightarrow c$ background; the projection plots for this step of the fit are presented in Fig. 2.

In the next step, we use the results obtained in the previous fit to extrapolate the predicted $b \rightarrow c$ background into the high p^* region ($p^* > 2.34$ GeV for K^+ and K_S^0 , $p^* > 2.36$ GeV for π^+). We fit these subsamples, varying only the yields of the signal and $q\bar{q}$ background components and the charge asymmetries, while the shapes are those determined in the previous step (see Fig. 3). An

exception occurs for the \mathcal{F} variable in the $q\bar{q}$ background, which is correlated with p^* ; thus, fixing its shape to that determined in the whole p^* range would lead to a bias. In this case we parameterize the \mathcal{F} distribution with two Gaussians, determine its parameters from the MC in the high p^* range, and leave the mean of the core Gaussian free to vary in the fit. Using the p^* cut efficiency derived from the MC, we then recalculate the number of signal events in the whole p^* range and repeat the fitting procedure from the beginning.

We find that this procedure converges after at most six cycles and that the result does not depend on the initial values we choose for the signal yield. We use the results of the final fit to the high p^* range to derive the partial branching fractions and the direct CP -asymmetries (for the K^+ and π^+ samples). The branching fractions are computed using the efficiencies for reconstructing signal events in the high p^* region derived from the simulation. In order to avoid the systematic uncertainty related to the B_{reco} reconstruction efficiency, the calculation is done taking for the normalization the number of $B\bar{B}$ events present in our sample. To make the comparison with the kaon samples easier, we extrapolate the branching fraction of $B \rightarrow \pi^+ X$ to the $p^* > 2.34$ GeV range (we assume the systematic error associated with this extrapolation to be negligible). The results are collected in Table I.

The whole fit procedure is tested on a data sample enriched in $b \rightarrow c$ background, selected by reversing the vetoes on the D^0 , D^+ , or D_s^+ candidates associated with the B_{sig} . The results agree within statistical uncertainties with the expectations of very small signal yields. We also verify that our model for the continuum background is in very good agreement with the data taken away from the $Y(4S)$ resonance.

Systematic uncertainties arise from the imperfect knowledge of the number of B_{reco} candidates (5%), from

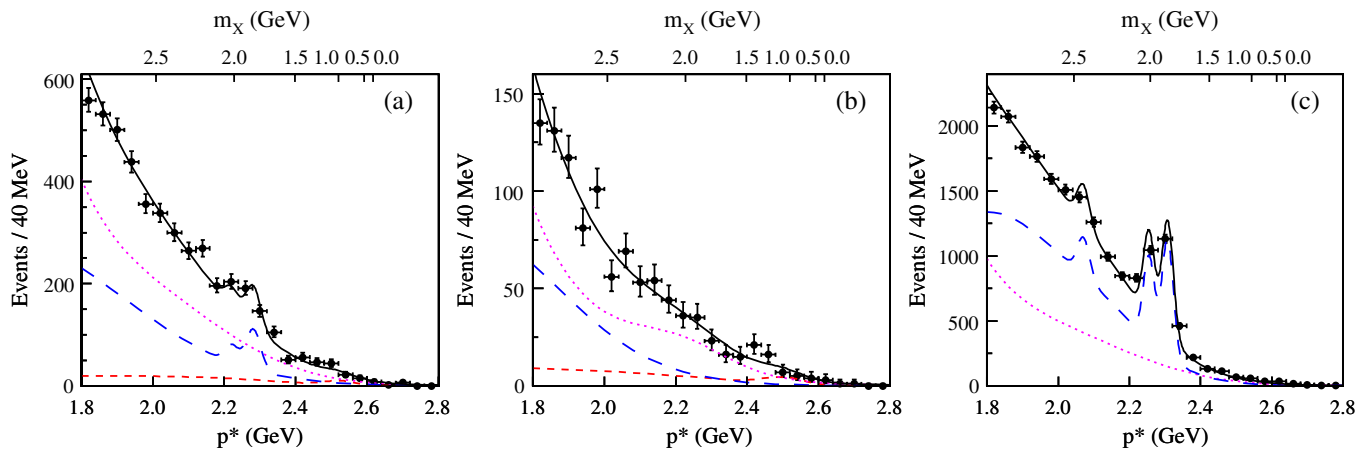


FIG. 2 (color online). Projection plots for the whole p^* range for the (a) K^+ , (b) K_S^0 , and (c) π^+ samples. The solid curves are the total fit functions, the (red) dashed lines are the signal components (which are kept fixed at this stage), the (blue) long dashed lines are the $b \rightarrow c$ background and the (magenta) dotted lines are $q\bar{q}$. The scale on the upper border of the plots indicates the mass of the system recoiling against the light hadron.

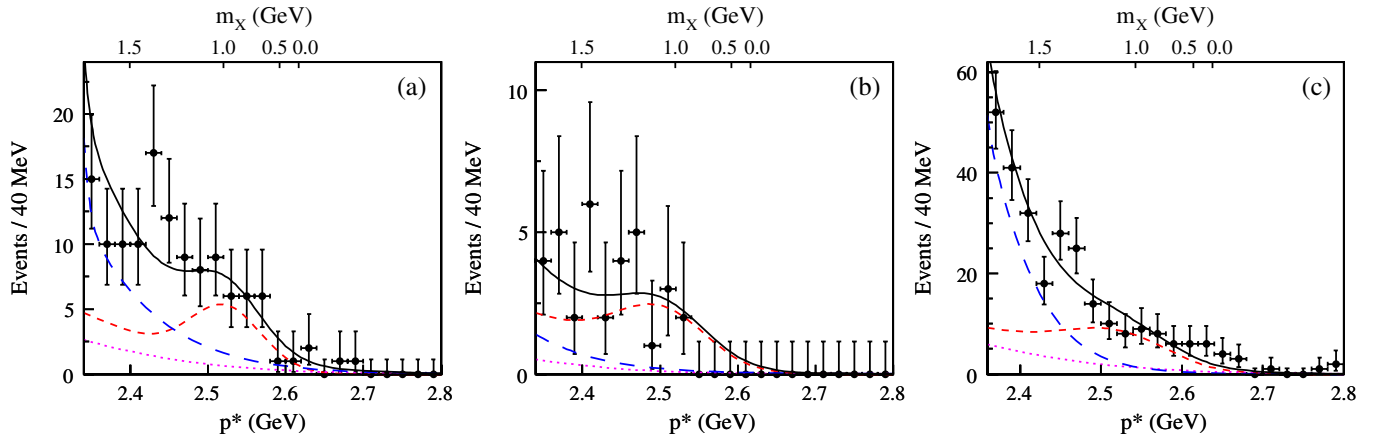


FIG. 3 (color online). Projection plots for $p^* > 2.34(2.36)$ GeV for the (a) K^+ , (b) K_S^0 , and (c) π^+ samples. The solid curves are the total fit function, the (red) dashed lines are the signal component, the (blue) long dashed are the $b \rightarrow c$ background and the magenta dotted are $q\bar{q}$. In order to enhance the signal component we apply cuts on the likelihood (computed excluding the p^* variable) which retain 82–88% of signal events while suppressing most of the $q\bar{q}$ background. The scale on the upper border of the plots indicates the mass of the system recoiling against the light hadron.

the uncertainties on the reconstruction efficiencies for charged particles (0.5%), K_S^0 candidates (2.1%), and other neutral particles (0.9–1.2%, depending on the final state), from the K/π separation (2.4%), and from the statistics of the MC sample which we use to compute the efficiency in reconstructing signal events (6.8–14.5%). The above uncertainties are multiplicative and do not affect the significance of the measured branching fractions, contrary to the following additive contributions: the uncertainty on the PDFs of the signal component is estimated by leaving each parameter kept fixed in the nominal fit free to vary (3.6–8.5 events). The uncertainty in the $b \rightarrow c$ background is computed by varying its yield by the sum in quadrature of its Poisson uncertainty and the uncertainty in the extrapolation to the high p^* region, taking into account the

uncertainty on the knowledge of the signal PDF. The resulting systematic error is 2.8–10.3 events. The systematic error arising from the correction for the fit bias is taken as the sum in quadrature of half the correction itself and the statistical uncertainty on the correction (3.6–7.9 events).

The systematic uncertainties for the direct CP asymmetries include the uncertainty in detector related charge asymmetries, which mainly affect the kaons (2%), different reconstruction efficiencies for B and \bar{B} candidates in the tag sample (2.5%), and effects due to mistagging (3%).

Our results for the partial branching fractions and \mathcal{A}_{ch} are given with statistical and systematic errors in Table I. The central values for the branching fractions are in agreement with our estimates [14] of the sums of the known exclusive branching fractions of charmless two- and

TABLE I. Summary of the fit results to the high p^* range. The $b \rightarrow c$ background yield is kept fixed in this fit; the quoted uncertainty represents the amount by which this quantity is varied for the evaluation of systematic uncertainties. The first error in the branching fractions and in the direct charge asymmetries is the statistical one, while the second is systematic (the significance includes only the additive part of the latter). The upper limits (U.L.) on the partial branching fractions are taken at the 90% confidence level. For the π^+ sample, the results of the yields refer to the $p^* > 2.36$ GeV range, whereas the branching fraction has been extrapolated to $p^* > 2.34$ GeV.

	$B \rightarrow K^+ X$	$B \rightarrow K^0 X$	$B \rightarrow \pi^+ X$
Events to fit	306	84	692
$b \rightarrow c$ yield (events)	66 ± 8	6.5 ± 2.6	173 ± 13
$q\bar{q}$ yield (events)	194 ± 15	48 ± 8	430 ± 22
Signal yield (events)	54^{+11}_{-10}	32^{+7}_{-7}	107^{+15}_{-14}
Fit bias (events)	+10.9	+3.5	-4.3
Significance (σ)	2.9	3.8	6.7
$\mathcal{B} (\times 10^{-6})_{p^* > 2.34 \text{ GeV}}$	$119^{+32}_{-29} \pm 37$	$195^{+51}_{-45} \pm 50$	$372^{+50}_{-47} \pm 59$
$\mathcal{B} \text{ U.L. } (\times 10^{-6})_{p^* > 2.34 \text{ GeV}}$	187	294	...
\mathcal{A}_{ch}	$0.57 \pm 0.24 \pm 0.05$...	$0.10 \pm 0.16 \pm 0.05$

three-body B decays. On the other hand, predictions based on SCET [4] underestimate the measurements, both those of the inclusive branching fractions presented here and those obtained by summing exclusive modes, even after adjusting for the branching fractions of the $B \rightarrow \eta^{(\prime)}X$ modes, which are acknowledged to be problematic for SCET. This fact is interpreted by the authors of Ref. [4] as an indication of the need to introduce substantial non-perturbative charming penguin contributions or large higher-order corrections.

In conclusion we have measured the inclusive partial branching fractions for $B \rightarrow K^+X$, $B \rightarrow K^0X$, and $B \rightarrow \pi^+X$ in the region where the momentum of the candidate hadron is greater than 2.34 GeV. The statistical significance, computed as the difference between the value of $-2\ln\mathcal{L}$ for the zero signal hypothesis and the value at its minimum, exceeds 5 standard deviations in each case; however, comparable systematic uncertainties lower the significance to the values quoted in the table, and we quote 90% confidence level upper limit (taken as the value below which lies 90% of the total of the likelihood integral, in the

region where the branching fraction is positive) for the K^+ and K^0 modes. We observe $B \rightarrow \pi^+X$ independently of previously reported observations of exclusive modes. All results are in agreement with the standard model predictions, and exclude large enhancements due to sources of new physics. We do not find any significant direct CP asymmetry in the K^+ and π^+ samples.

We are grateful for the excellent luminosity and machine conditions provided by our PEP-II colleagues, and for the substantial dedicated effort from the computing organizations that support *BABAR*. The collaborating institutions wish to thank SLAC for its support and kind hospitality. This work is supported by DOE and NSF (USA), NSERC (Canada), CEA and CNRS-IN2P3 (France), BMBF and DFG (Germany), INFN (Italy), FOM (The Netherlands), NFR (Norway), MES (Russia), MICIIN (Spain), STFC (United Kingdom). Individuals have received support from the Marie Curie EIF (European Union), the A.P. Sloan Foundation (USA) and the Binational Science Foundation (USA-Israel).

-
- [1] C. Greub and P. Liniger, *Phys. Rev. D* **63**, 054025 (2001).
 [2] I. Bigi *et al.*, *Phys. Lett. B* **323**, 408 (1994).
 [3] A. Goksu, E. O. Iltan, and L. Solmaz, *Phys. Rev. D* **64**, 054006 (2001).
 [4] J. Chay, C. Kim, A. K. Leibovich, and J. Zupan, *Phys. Rev. D* **76**, 094031 (2007).
 [5] H. Davoudiasl and E. Ponton, *Phys. Lett. B* **680**, 247 (2009).
 [6] A. Lenz, U. Nierste, and G. Ostermaier, *Phys. Rev. D* **56**, 7228 (1997).
 [7] T. E. Browder, K. Honsheid, and D. Pedrini, *Annu. Rev. Nucl. Part. Sci.* **46**, 395 (1996); B. Barish *et al.* (CLEO Collaboration), *Phys. Rev. Lett.* **76**, 1570 (1996); H. Albrecht *et al.* (ARGUS Collaboration), *Phys. Lett. B* **318**, 397 (1993).
 [8] A. Czarnecki, M. Slusarczyk, and F. Tkachov, *Phys. Rev. Lett.* **96**, 171803 (2006).
 [9] H. Albrecht *et al.* (ARGUS Collaboration), *Phys. Lett. B* **353**, 554 (1995); T. E. Coan *et al.* (CLEO Collaboration), *Phys. Rev. Lett.* **80**, 1150 (1998); P. Abreu *et al.* (DELPHI Collaboration), *Phys. Lett. B* **426**, 193 (1998).
 [10] Unless otherwise stated, charge conjugate reactions are implied throughout the paper.
 [11] B. Aubert *et al.* (*BABAR* Collaboration), *Nucl. Instrum. Methods Phys. Res., Sect. A* **479**, 1 (2002).
 [12] H. Albrecht *et al.* (ARGUS Collaboration), *Phys. Lett. B* **241**, 278 (1990).
 [13] The *BABAR* detector Monte Carlo simulation is based on GEANT4, S. Agostinelli *et al.*, *Nucl. Instrum. Methods Phys. Res., Sect. A* **506**, 250 (2003) and EvtGen and D. J. Lange, *Nucl. Instrum. Methods Phys. Res., Sect. A* **462**, 152 (2001).
 [14] Our rough estimate of the summed two- and three-body B decay branching fractions is based on the world average values in Particle Data Group, C. Amsler *et al.*, *Phys. Lett. B* **667**, 1 (2008).